Materials Research. 2022; 25:e20220186
DOI: https://doi.org/10.1590/1980-5373-MR-2022-0186

Green Polyethylene in Harsh Environments: Gamma-irradiation Effects

Pablo R. de Medeiros[a], Patricia L. B. Araujo[a,b], Katia A. S. Aquino[a,c], Elmo S. Araujo[a]*

[a]*Universidade Federal de Pernambuco (UFPE), Departamento de Energia Nuclear, Av. Prof. Luiz Freire, 1000, Cidade Universitária, 50740-545, Recife, PE, Brasil.*
[b]*Universidade Federal de Pernambuco (UFPE), Departamento de Engenharia Biomédica, Av. Jornalista Anibal Fernandes, s/n, Área II, Cidade Universitária, 50740-560, Recife, PE, Brasil.*
[c]*Colégio de Aplicação da UFPE, Av. da Arquitetura, s/n, Cidade Universitária, 50740-550, Recife, PE, Brasil.*

Received: April 5, 2022; Revised: July 24, 2022; Accepted: July 28, 2022

Bio-based linear low-density polyethylene (green LLDPE) composites are used as electrical jackets/insulator for cables. Assessments of gamma-irradiation (Co-60) effects on these materials are of interest as they might be used in nuclear power plants (NPPs). Brazilian sugarcane juice-based green LLDPE composite electrical jackets were irradiated until 1000 kGy and analyzed for thermal stability and mechanical characteristics. Thermogravimetry analysis (TGA) showed increasing of pyrolysis activation energy (E_a) (under N_2) from 42.7 ± 4.2 kJ/mol in unirradiated samples to 72.8 ± 4.6 kJ/mol after 60 kGy dose, as resulted of radiation-induced effects. FTIR spectra evidenced radiation-induced formation of conjugated C=C bonds after 250 kGy dose. Tensile stress and Young modulus did not change significantly until 150 kGy dose, whereas elongation at break decreased and reached 50% at 91 kGy dose. These results suggest that green LLDPE might withstand radiation damage through a NPP operating life (~ 40 years).

Keywords*: bio-based plastics, gamma radiation, LLDPE thermal properties, LLDPE mechanical properties, nuclear power plants.*

1. Introduction

Bio-based plastics are materials made from renewable resources[1]. The replacing of non-renewable with renewable resources is a key item on several organizations, also it is the subject of many public and private debates. Thus, renewable resources have become an economically viable alternative to traditional materials[2-4]. They are very attractive materials as alternatives to fossil-based polymers, especially when used as large-scale commodity plastics. Research on conventional or new polymers made from renewable resources has exponentially expanded worldwide[1] and some products have reached the shelves[1,5-7].

Green plastics differ from traditional plastics in terms of sustainability, since they help reduce greenhouse gas (GHG) emissions along the production chain. The cultivation of sugarcane, which sources green polyethylene (PE) production, also aids in the capture and sequestration of carbon, which contribute to climate change mitigation. From sugarcane cultivation to the production of green PE, each kilogram of green polyethylene produced captures about 3.09 kilos of CO_2 (the life cycle assessment of green PE), which is a calculation that considers the CO_2 gains and losses in all stages of the production process[2]. The importance of green plastic is demonstrated in a comparison to previous data on naphtha, a traditional polyethylene. Green PE is the first certified plastic made from a renewable source worldwide, making the petrochemical industry a pioneer in this field. However, green plastic is not necessarily a biodegradable polymer, since they have a long time to degrade in natural environment compared to biodegradable plastics. Green production of plastic materials arise new concepts, as sustainable supply-chain management (SSCM). SSCM, in general, involves aspects of business sustainability (economy, society, environment, etc.) and supply-chain management (SCM)[8,9]. Thus, debates on innovation, sustainable development (SD) and SSCM provide information for modifications on petrochemical production chain strategy, recently, that include the use of raw materials, as renewable energy, for green plastic production[10,11]. In addition, the concept of sustainable development include the idea that social, economic and environmental problems should be analyzed jointly, allowing for interfacing[12-16].

Most commercial bio-based polymers derive from agricultural feedstocks such as sugarcane, corn or potatoes. Afumex® green, a chlorine-free flexible cable (Prysmian -Brazil), is commercialized as having biopolyethylene produced from sugar obtained from sugarcane juice as electrical jacket and insulation materials.

Jacket or insulation materials used in electrical cables and wires are frequently made of polymer composites containing large quantities of flame retardant compound, for instance EVA jacket contain ~40°wt% of $Al(OH)_3$[17], and additives as stabilizers and pigment. Older Nuclear Power Plant (NPP) facilities use poly(vinyl chloride) (PVC) coated wirings[18,19]. Other protective polymers include crosslinked polyethylene

* e-mail: elmo.araujo@ufpe.br

(XLPE, ethylene-propylene-based elastomers (EPR, EPDM), chlorosulphonated polyethylene (CSPE), or poly(ethylene vinyl acetate) (EVA)[20]. In modern NPPs, halogen-free cable and wire materials are preferred as there are concerns about toxic fume emissions in the event of a fire[20].

Polyethylene is known for undergoing crosslinking when exposed to ionizing radiation, due to its molecular structure to be prone for this radiolytic effect[21-23]. Catari and co-workers[24] observed long-chain branching and/or crosslinking effects on gamma-irradiated neat linear low-density polyethylene (LLDPE) at dose range of 15 – 200 kGy, by melt flow index (MFI) measurements. MFI decreases with increasing absorbed dose, which indicates formation of crosslinking between main chains. This effect promoted reduction in initial degradation temperatures (T_{onset}) and activation energy (E_a) at higher doses (100 and 200 kGy), which characterizes thermal stability decrease of the polymer material[24].

In this work, we assessed radiolytic effects on commercial polymer composites fabricated with green LLDPE. Thermal and mechanical evaluations performed in these composites exposed to up to 1000 kGy absorbed dose suggested that they are radiostable enough to withstand service conditions in NPPs, thus, presenting good potential as materials for electrical cable jackets/insulators.

2. Experimental

2.1 Sample Preparation and Gamma Irradiation

Electrical cables (Afumex™ Green - PRYSMIAN –BRAZIL)[25] with 4 mm^2 nominal cross-section, isolation tension of 450/750 V were cut into 1m long pieces, winded and braced to fit the irradiator chamber (non-attenuated ^{60}Co source Gammacell GC220 Excel irradiator - MDS Nordion, Canada). Irradiation doses were of 60, 250, 500, and 1000 kGy in air, dose rate of 0.61 $Gy.s^{-1}$, at room temperature (~ 300 K).

In this work, a green LLDPE grade SLH218 was used. It is a LLDPE hexene copolymer. It shows a good balance between optical properties, mechanical properties, sealability and processability. Very low gel content. The minimum biobased carbon content of this grade is 84%, according to the supplier. It is used in medium and low voltage insulation of electrical wire and cables.

After irradiation, the cables were cut into 150 mm long pieces, slited lengthwise with a craft knife, and jacket/insulator sleeves were carefully stripped off with minimum deformation. For tensile testing the sample dimension was 4 mm width, 50 mm length at measurement area, following Boguski et al[17].

2.2 Thermal Analysis

Termogravimetry Analysis (TGA) (Simultaneous TGA/DSC2 STARe thermoanalyzer- Mettler Toledo-Switzerland) in jacket/insulator sleeves was done in 70 microliters aluminum oxide crucibles, under N_2 (~99.5%) or O_2 (~99.5%) atmosphere (50 $mL.min^{-1}$ flux), heating rates of 10, 30 or 50 $°C.min^{-1}$ in the 30-500 °C temperature range.

2.2.1 Activation energy (E_a) calculations by isoconversion methods

A wide range of methods for calculating the activation energy (E_a) of pyrolysis reactions were proposed[26-36]. Some of these methods require the determination of temperatures at which an equivalent stage of the pyrolysis reaction takes place for different heating rates (β), and are called isoconversion methods. The equivalent stage, also called fixed or identical stage, is defined as the stage at which a fixed amount or a fixed fraction of the total amount is transformed[26].

In general, it is assumed that conversion rate (Ω) during a pyrolysis reaction is the product of two functions: conversion fraction *f(x)* and temperature *k(T)* according to Equation 1[26].

$$\Omega = \frac{dx}{dt} = f(x)k(T) \tag{1}$$

k(T) is a temperature dependent function that usually follow an Arrhenius-type equation:

$$k = k_0 \exp(-E_a / RT) \tag{2}$$

where k_0 is a coefficient that depends on pyrolysis reaction kinetic model; E_a is the activation energy, and *R* is the universal gas constant (0.0304 $J.mol^{-1}.°C^{-1}$).

Conversion fraction *x* is given by Equation 3:

$$x = \frac{w_0 - w_t}{w_0 - w_f} \tag{3}$$

where w_0 and w_f are sample weights at the beginning and at the end of the observed weight loss event, respectively, and w_t is the sample weight at a given time *t*.

Some isoconversion methods are based on mathematical approximation of the temperature integral, as given in Equation 4. Here, we use isoconversion methods which require data on T_f(β) only. These integral methods are named *p(y)*-isoconversion methods[27].

$$\int_0^x \frac{dx}{f(x)} = \frac{k_0}{\beta}\int_0^{T_f} \exp(-E_a / RT)dT = \frac{k_0 E_a}{\beta R}\int_{y_f}^{\infty} \frac{\exp(-y)}{y^2}dy \tag{4}$$

where $y = E_a/RT$; $y_f = E_a/RT_f$; T_f is the temperature at an equivalent (fixed) state of transformation; and β is the heating rate (*dT/dt*).

p(y)-isoconversion methods replace the Arrhenius integral (Equation 4), right side) by mathematical approximations, regardless the type of *f(x)*. In other words, these methods are independent of the mathematical model assumed for the transformation reaction kinetics used to calculate E_a [27]. Thus, for simplicity, we isolated the temperature integral from Equation 4:

$$p(y_f) = \int_{y_f}^{\infty} \frac{\exp(-y)}{y^2}dy \tag{5}$$

Mathematical approximations for Equation 5 follow a general approximation model described by:

$$p(y) \cong \frac{\exp(-Ay + B)}{y^k} \tag{6}$$

Here, the values of *k*, *A* and *B* can be optimized by minimizing the deviation between the approximation function and the

exact integral[27]. By taking the logarithm of Equation 4 and using Equation 6 one obtains:

$$\ln\int_0^x \frac{dx}{f(x)} = \ln(\frac{k_0 E_a}{R}) + \ln(\frac{1}{\beta y_f^k}) - A y_f + B \quad (7)$$

This leads to the Equation 8, at constant conversion fraction x[27]:

$$\ln(\frac{\beta}{T_f^k}) = -A\frac{E_a}{RT_f} + C \quad (8)$$

E_a is easily determined from the slope of the $\ln(\beta / T_f^k)$ *versus* $1/T_f$ curve. C is a constant independent of T and β, and R is the universal gas constant (0.0304°J.mol^{-1}.°C^{-1}). Table 1 shows three traditional isoconversion methods and their mathematical approximations of Arrhenius integral to determine E_a from Equation 8.

In this work, to calculate E_a we used the Starink method which performed the integral-mathematical approximation on the best accuracy[27].

The methods presented into Table 1 are all independent from pyrolysis reaction kinetic model, i.e., function *f(x)*. Have been reported by some researchers[37-39] which pyrolysis reaction mechanisms might changing with different heating rates, leading to shifts in TGA curves. In addition, inefficient heat transfer may produce large differences between furnace and sample temperatures. Alterations in thermal data with heating rate might also be caused by the random nature of pyrolysis processes[40]. Thus, the use of pyrolysis kinetic model-independent isoconversion methods is a suitable way of circumventing such hurdles.

2.3 Fourier Transform Infrared (FTIR) Spectroscopy Analysis

FTIR analysis were performed in a FTIR-4600 Jasco Spectrometer (Japan) equipped with an Attenuated Total Reflection (ATR ProOne) accessory, ZnSe crystal, incident angle 45º in the center, circular contact area of 4.9 mm^2. Experiments were run in 32 scans, at 4 cm^{-1} resolution, in the 4000-400 cm^{-1} wavenumber range, under normal atmosphere.

2.4 Tensile testing

Samples were tested in quadruplicate for mechanical performance (Shijin WDW-E Mechanical Tester, Jinan Time Trial Testing Machine Co. China), in order to evaluate gamma irradiation effects on green LLDPE jacket/insulator. Tests were performed at room temperature (~300 K), using crosshead speed of 50 mm.min^{-1}. Tensile stress (TS), Elongation (E% = [(L-L_0)/L_0]100, L_0 and L are the original and at any time distance between gage marks, respectively) and Young Modulus (YM) was determined according to ASTM D1248[41] and ASTM D638[42].

3. Results and Discussion

3.1 Thermal degradation of LLDPE

Figure 1 show TGA and DTGA thermograms of unirradiated green LLDPE composites (heating rate of 10 °C.min^{-1}) under N_2 or O_2 atmospheres. It is clear that pyrolysis reactions are accelerated by oxygen. The thermal parameters: T_{onset} (initial degradation temperature), T_{max} (maximum-rate degradation temperature) were lower in experiments under O_2 flux, whereas R_{max} (mass-loss maximum rate) presented value higher compared to samples assayed in N_2 (Table 2).

Figure 2 shows thermogravimetry analysis (TGA) for unirradiated and gamma-irradiated green linear low density polyethylene (LLDPE) composite carried out at 10 °C.min^{-1} heating rate under N_2 and O_2 atmospheres.

The influence of O_2 atmosphere in decreasing thermal stability leads pyrolysis to occur at lower temperatures and in a much faster way. R_{max} values are at least 5.8 times

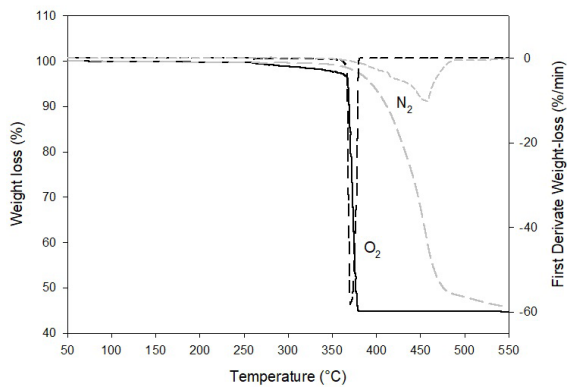

Figure 1. Thermogravimetry and Differential Thermogravimetry analysis (TGA and DTGA, respectively) results for unirradiated green linear low density polyethylene (LLDPE) composite carried out at 10 °C.min^{-1} heating rate, under O_2 and N_2 atmospheres.

Table 1. Parameters *A* and *k* from Equation 8 for *p(y)*-isoconversion methods.

Method	*p(y)*-approximation	*A*	*k*	*Reference*
Starink	Starink $p(y) \cong \frac{\exp(-1.008y - 0.312)}{y^{1.92}}$	1.008	1.92	27
Kissinger-Akahira-Sunose (KAS)	Murray and White $p(y) \cong \frac{\exp(-y)}{y^2}$	1	2	28-30
Flynn-Wall-Ozawa (FWO)	Doyle $p(y) \cong \exp(-1.0518y - 5.330)$	1.0518	0	31-35

Table 2. Thermal degradation parameters of unirradiated or gamma-irradiated LLDPE at 60 kGy or 250 kGy dose in O_2 or N_2 atmospheres. Heating rate of 10 °C.min^{-1}.

Atmosphere	Dose (kGy)	T_{onset} (°C)	T_{max} (°C)	R_{max} (% mass- loss. min^{-1})	Entry
Nitrogen	unirradiated	384	457	10	1
	60	390	462	12	2
	250	391	461	12	3
Oxygen	unirradiated	368	371	58	4
	60	374	376	113	5
	250	384	398	60	6

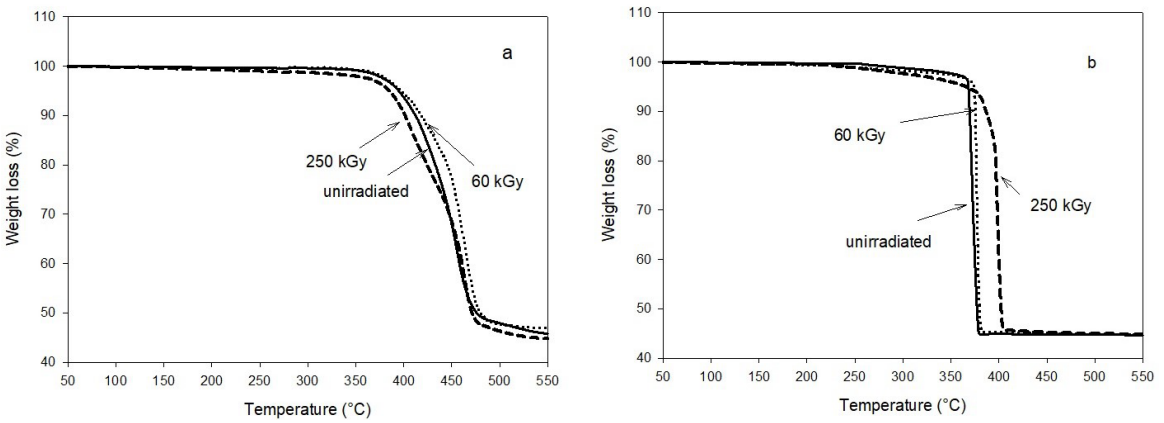

Figure 2. Thermogravimetry analysis (TGA) results for unirradiated and gamma-irradiated green linear low density polyethylene (LLDPE) composite carried out at 10 °C.min^{-1} heating rate under a) N_2 and b) O_2 atmospheres.

higher for samples assayed under O_2 in all absorbed doses, highlighting the strong influence of oxidative processes. On the other hand, it is noted that gamma-irradiation does not markedly change the thermal parameters (T_{onset}, T_{max}, R_{max}) of LLDPE under N_2 flux (without oxidative process) (Table 2, Entry 1-3). Nevertheless, TGA experiments of LLDPE under O_2 flux at 250 kGy dose, show some increase in thermal stability in comparison with unirradiated samples, as T_{onset} and T_{max} are lower for the later (Table 2, Entries 4 and 6), suggesting increase in molecular structure stability, possibly due to elimination reactions of oxygenated side groups by radiolysis, followed by formation of less labile groups, such as main chain conjugated double bonds (see section 3.3) or crosslinking reactions[21]. Figure 2b shows that T_{max} shifts toward higher temperature when samples are irradiated at 250 kGy under O_2, suggesting that radiation-induced crosslinking structures difficult the thermo-oxidative process which take place on polymer system.

Catari et al.[24] investigated radiation-induced crosslinking effects on neat LLDPE at dose range of 15 – 200 kGy, by Melt Flow Index (MFI) measurements. They did not observe significantly change in T_{onset} and E_a in pyrolysis reactions (under N_2 flux) for neat LLDPE at dose up to 50 kGy, but at doses of 100 and 200 kGy, these parameters decreased 7% and 18%, respectively, probably due to crosslinking excess.

In contrast, radiation-induced crosslinking reactions might also promote increase in thermal stability of LLDPE composites, which seems to be the case in this work. In fact, radiation-induced crosslinking and main chain scissions effects depend on molecular structure of the polymer, but industrial processing features also influence on the predominance of one effect over the other.

3.2 Activation energy calculations

Activation energy (E_a) for LLDPE was calculated by Starink method using TGA data, at the heating rates of 10, 30, and 50 °C.min^{-1}. Figure 3 shows plot ln ($\beta/T^{1.92}$) *versus* 1/T for unirradiated LLDPE, at single conversion rate of 0.5. Here, by straight-line declination, it was possible to obtain of 41.8 kJ/mol and 40.4 kJ/mol for E_a at N_2 and O_2 flux respectively. Additionally, values of E_a for different conversion fraction *x* (0.2 – 0.8) for unirradiated green LLDPE (under N_2 and O_2) were determinate (Table 3).

Average E_a values determined for unirradiated LLDPE were 42.7 ± 4.2 (under N_2) and 40.1 ± 2.0 (under O_2) kJ.mol^{-1}. These values are in agreement with the literature, which presented values in the range 63 to 75 kJ.mol^{-1} measured for several thermally-aged cable materials[43]. It is worth noting that thermo-oxidative processes did not significantly affect E_a. However, activation energy increased from 42.7 kJ.mol^{-1} to 72.8 kJ.mol^{-1} and 67.0 kJ.mol^{-1}, when LLDPE composite is irradiated with 60 kGy and 250 kGy, respectively, in TGA experiments at N_2 flux (Table 4). This increasing of ~70% on E_a values in doses of 60 and 250 kGy were attributed to radiation-induced crosslinking effects which improved polymer-matrix thermal stability. Similar effects were observed

in irradiated neat polyimide (PI) with protons (62 MeV) at dose rage of 10 – 80 kGy[44]. In contrast, Catari et al.[24] pointed out no significant changes in E_a for gamma-irradiated LLDPE at doses of 15 – 50 kGy, and decrease in E_a at doses of 100 and 200 kGy. In addition, E_a under O_2 also increased for gamma-irradiated LLDPE composite with values of 40.1 kJ.mol^{-1} (unirradiated), 51.4 kGy (60 kGy), and 112.5 kGy (250 kGy).

Table 3. Activation energy (E_a) at conversion fraction *x* (0.2 – 0.8) for unirradiated green LLDPE. TGA experiments carried out at 10, 30 and 50 °C.min^{-1} heating rates under N_2 and O_2 atmospheres, by using Starink method[27].

Conversion *x*	E_a (kJ/mol) N_2	E_a (kJ/mol) O_2
0.2	39.5	43.1
0.3	38.2	41.5
0.4	38.7	41.0
0.5	41.8	40.4
0.6	44.7	39.1
0.7	47.1	38.2
0.8	48.8	37.4
	42.7 ± 4.2	40.1 ± 2.0

Table 4. Average activation energy, E_a, calculated by isoconversion Starink method[27] at heating rates of 10, 30 and 50 °C.min^{-1}, at conversion fraction x of 0.2 – 0.8.

Atmosphere	Dose (kGy)	Activation energy (kJ.mol^{-1})	Entry
Nitrogen	0	42.7 ± 4.2	1
	60	72.8 ± 4.6	2
	250	67.0 ± 1.7	3
Oxygen	0	40.1 ± 2.0	4
	60	51.4 ± 3.4	5
	250	112.5 ± 11.6	6

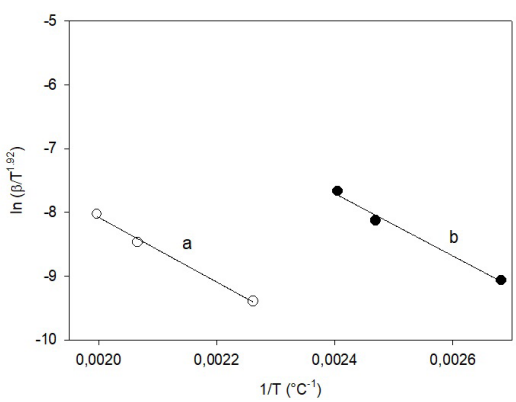

Figure 3. Calculation of activation energy by Starink method from plot ln ($\beta/T^{1.92}$) *versus* 1/T come from thermogravimetry analysis (TGA) for unirradiated LLDPE composite carried out at 10, 30 and 50 °C.min^{-1} heating rates (β) and conversion rate x = 0.5 only, under a) ○ N_2 (E_a = 41.8 kJ/mol; r^2 = 0.995) and b) ● O_2 (E_a = 40.4 kJ/mol, r^2 = 0.989) atmospheres.

3.3 FTIR spectroscopy analysis

FTIR spectra of unirradiated or irradiated green LLDPE are shown in Figure 4. Absorption bands attributed to LLDPE could be seen peaks at 2916 and 2848 cm^{-1} corresponding, respectively, to asymmetric and symmetric stretching of -CH_2- groups, the peak at 1434 cm^{-1} assigned to bending vibrations of -CH_2-, and the peak at 715 cm^{-1} assigned to inner rocking vibration of -CH_2- in the amorphous polymer phase. In contrast, the strong and sharp peak at 3693 cm^{-1}, attributed non-hydrogen bonding hydroxyl stretching vibration might come from additives or fillers, such as hydrated aluminum oxide. Carbonyl stretching at (1734 cm^{-1}), and C-O stretching vibrations (around 1100 cm^{-1}, also present in FTIR spectrum are probably from additives, as well.

High energy ionizing radiation causes alterations in the polymer chemical structure through mechanisms like crosslinking, chain scission, oxidation, and/or formation of double bonds[45-47]. Figure 5 shows some these mechanisms on irradiated polyethylene suggested by Bracco et al.[47]. In FTIR spectrum of gamma-irradiated green LLDPE, a peak at 1585 cm^{-1} assigned to C=C bond was identified. In general, C=C peaks appear in higher wavenumber (from 1640 to 1670 cm^{-1}), but when C=C is conjugated, an intense peak appears in lower wavenumber[48]. This implies that conjugated double bonds are generated after gamma irradiation on green LLDPE, as a result of elimination reactions of allyl hydrogens.

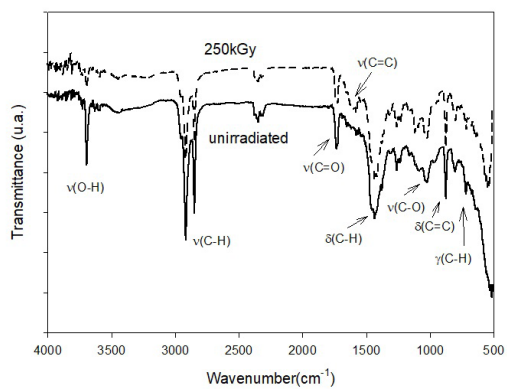

Figure 4. FTIR spectra of unirradiated or gamma-irradiated at 250 kGy green LLDPE (jacket outer surface) in air, at room temperature.

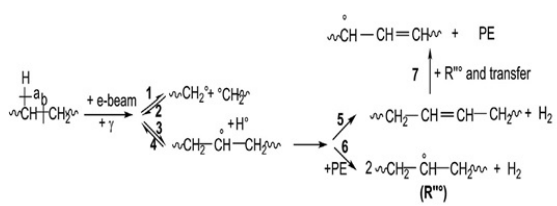

Figure 5. Initiation reaction by high energy radiation on polyethylene. Adapted from Bracco el at[47].

3.4 Tensile testing

According to Charlesby[21], linear polymers with structural units of (-CH_2-C(R)H-), i.e. hydrogen atoms bonded to tertiary carbons have higher probability to undergo crosslinking under ionizing irradiation. C-H bond is broken by loss of a binding electron, resulting in radical structures and consequent crosslinking between main chains. As a result, crosslinking frequently promotes increase in Young Modulus (YM) and tensile stress properties by increasing molecular stiffness. However, radiation-induced effects on polymer composites used in applications as cable and wire jackets/insulator are complex phenomena. Green LLDPE composite samples investigated in the present work are used as jackets for low voltage power wiring (< 1 kV). In addition, these jackets contain additives, such as fillers, antioxidants, stabilizers, flame retardants or pigments that might influence in mechanical behavior of the polymer matrix. Figure 6 shows YM and tensile stress properties as a function of absorbed gamma radiation dose on green LLDPE. No significant changes in these properties are observed for gamma-irradiated green LLDPE until 150 kGy. It is quite probable that additive components present in the polymer composite system promote some radiolytic stabilization in the molecular structure. After 150 kGy, both mechanical properties drastically decrease, due the high intensity of gamma radiation energy transferred to the polymer system, causing radiolytic degradation.

In general, elongation at break is the benchmark property to assess suitable low-voltage power cable performance in NPPs, since the structural integrity of the material, and therefore its functionality, is usually verified through its elasticity over time[45]. For monitoring the mechanical degradation induced by aging for radiation and/or heat exposure in the NPPs environment, it is recommend the evaluation of elongation at break as a function of irradiation dose and temperature. Current standards suggest that elongation values of 50%, absolute or relative, must be used to define electrical cables and wire end-of-life[49]. Electrical cables and wires These components used in NPPs are exposed to gamma irradiation in dose rate of approximately 0.3 10^{-4} Gy/s (or 1 kGy/year)[50]. A NPP has an average 40 years operation lifetime, which gives an absorbed dose of ~ 40 kGy in all material under these operation conditions. However, accelerated ageing tests are performed in order to monitor mechanical cable degradation. In general, ageing studies are carried out at higher temperatures and/or higher dose rates than those seen in actual operation services[49].

Figure 7 shows elongation at break as a function of absorbed dose for "green" LLDPE composites. Experimental data of elongation at break *versus* irradiation dose fitted properly to an exponential model with parameters shown in Table 5. Thus, 60.9% elongation at break is 50% of elongation of unirradiated sample that corresponds to absorbed dose of ~ 91 kGy, following the exponential model fitted for the experimental data. Thus, 91 kGy is the dose to equivalent damage (DED) for green LLDPE elongation at break decrease to 50% of the initial value (unirradiated sample). This absorbed dose correspond to as twice as

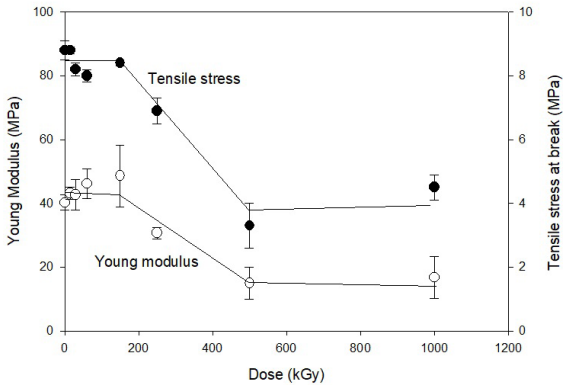

Figure 6. Young modulus and Tensile stress *versus* absorbed dose for gamma-irradiated green LLDPE composite in air, at room temperature.

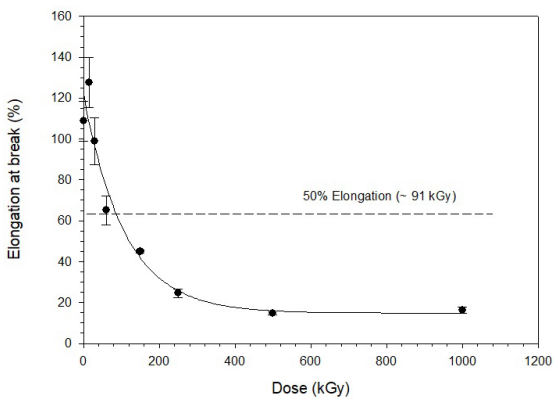

Figure 7. Elongation at break *versus* absorbed dose for gamma-irradiated green LLDPE composite in air, at room temperature.

Table 5. Statistic parameters of the exponential model for elongation versus dose fit.

Mathematical function	y_0	a	b	r^2
$y = y_0 + a.e^{(-bx)}$	14.821±8.387	107.037±11.079	0.009±0.003	0.949
Statistical tests				
Normality test (Shapiro-Wilk)		Passed (P = 0.2564)		
W Statistic = 0.8943 Significance level (<0.0001)				
Constant variance test		Passed (P = 0.0096)		

much of a NPP operation lifetime (~ 40 years). Therefore, green LLDPE composites have great potential as jacket and insulation of electrical cables and wire, directly competing with CSPE, EVA, PVC, and others, as jacket material used in nuclear power plants. It is understandable that the dose rate of ~0.61 $Gy.s^{-1}$ used on this work, in accelerated studies, is higher than that observed in actual service conditions (~0.3 10^{-4} $Gy.s^{-1}$). However, the value of elongation at break obtained with gamma irradiation accelerated ageing is a good approach to evaluate the reduction of elongation at 50% absolute value recommended by IAEA[49].

4. Conclusion

Gamma irradiation of green LLDPE composites promoted increase in activation energy (E_a) of pyrolysis reaction under O_2 or N_2 atmosphere. Maximum degradation rate (R_{max}) under O_2 was 5.8 times higher than N_2 atmosphere. Combined effects of oxidative processes and radiolytic events on green LLDPE composites were observed, with shift to higher initial degradation temperature (T_{onset}) and E_a at absorbed dose of 250 kGy.

FTIR spectrum of gamma-irradiated green LLDPE presented a new peak attributed to stretching vibrations of conjugated C=C bonds (1585 cm^{-1}). Tensile stress and Young Modulus did not change significantly until dose of 150 kGy, indicating that additive components might promote radiolytic stability. On the other hand, elongation at break decreased exponentially with increasing absorbed dose. Elongation at 50% absolute of initial value (unirradiated sample) was reached at 91 kGy (dose to equivalent damage), suggesting that green LLDPE composite electrical jackets/insulators have a good potential to be used in wiring material in nuclear power plants.

Acknowledgments

The authors would like to thanks to the National Council for Scientific and Technological Development - CNPq by financial support (grant numbers: 308417/2013-5).

References

1. Babu RP, O'Connor K, Seeram R. Current progress on bio-based polymers and their future trends. Prog Biomater. 2013;2(1):1-16. http://dx.doi.org/10.1186/2194-0517-2-8.
2. Vargas Mores G, Finosschio CPS, Barichello R, Pedrozo EA. Sustainability and innovation in the Brazilian supply chain of green plastic. J Clean Prod. 2018;177:12-8. http://dx.doi.org/10.1016/j.jclepro.2017.12.138.
3. Córdoba de Torresi SI, Pardini VL, Ferreira VF. Biomassa renovavel e o futuro da indústria química. Quim Nova. 2008;31(8):1923. http://dx.doi.org/10.1590/S0100-40422008000800001.
4. Silvestre BS. Sustainable supply chain management in emerging economies: environmental turbulence, institutional voids and sustainability trajectories. Int J Prod Econ. 2015;167:156-69. http://dx.doi.org/10.1016/j.ijpe.2015.05.025.
5. Mitsubishi Chemical Group. New Bio-based Engineering Plastic DURABIO™ [Internet]. 2020 [cited 2020 Aug 5]. Available from: https://www.m-chemical.co.jp/en/products/departments/mcc/sustainable/product/1201026_7964.html
6. Vink ETH, Glassner DA, Kolstad JJ, Wooley RJ, O'Connor RP. The eco-profiles for current and near-future NatureWorks® polylactide (PLA) production. Ind Biotechnol. 2007;3(1):58-81. http://dx.doi.org/10.1089/ind.2007.3.058.
7. Braskem. I'm green™ polyethylene [Internet]. 2020 [cited 2020 July 5]. Available from: http://www.braskem.com/site.aspx/Im-greenTM-Polyethylene
8. Ahi P, Searcy C. A comparative literature analysis of definitions for green and sustainable supply chain management. J Clean Prod. 2013;52:329-41. http://dx.doi.org/10.1016/j.jclepro.2013.02.018.
9. Diabat A, Kannan D, Mathiyazhagan K. Analysis of enablers for implementation of sustainable supply chain management: a textile case. J Clean Prod. 2014;83:391-403. http://dx.doi.org/10.1016/j.jclepro.2014.06.081.
10. Hall J, Matos SV, Martin MJ. Innovation pathways at the base of the pyramid: establishing technological legitimacy through social attributes. Technovation. 2014;34(5):284-94. http://dx.doi.org/10.1016/j.technovation.2013.12.003.
11. Hansen EG, Grosse-Dunker F, Reichwald R. Sustainability innovation cube: a framework to evaluate sustainability-oriented innovations. Int J Innov Manage. 2009;13(04):683-713. http://dx.doi.org/10.1142/S1363919609002479.
12. Iyer-Raniga U, Treloar G. A context for participation in sustainable development. Environ Manage. 2000;26(4):349-61. http://dx.doi.org/10.1007/s002670010092.
13. Giddings B, Hopwood B, O'Brien G. Environment, economy and society: fitting them together into sustainable development. Sustain Dev. 2002;10(4):187-96. http://dx.doi.org/10.1002/sd.199.
14. Hopwood B, Mellor M, O'Brien G. Sustainable development: mapping different approaches. Sustain Dev. 2005;13(1):38-52. http://dx.doi.org/10.1002/sd.244.
15. Boons F, Montalvo C, Quist J, Wagner M. Sustainable innovation, business models and economic performance: an overview. J Clean Prod. 2013;45:1-8. http://dx.doi.org/10.1016/j.jclepro.2012.08.013.
16. Carvalho AP, Barbieri JC. Innovation and sustainability in the supply chain of a cosmetics company: a case study. J Technol Manag Innov. 2012;7(2):144-56. http://dx.doi.org/10.4067/S0718-27242012000200012.
17. Boguski J, Przybytniak G, Łyczko K. New monitoring by thermogravimetry for radiation degradation of EVA. Radiat Phys Chem. 2014;100:49-53. http://dx.doi.org/10.1016/j.radphyschem.2014.03.028.
18. Gazdzinski RF, Denny WM, Toman GJ, Butwin RT. Ageing management guideline for commercial nuclear power plants: electrical cable and terminations. Albuquerque: Sandia National Labs for the US Department of Energy; 1996. (Report SAND; 96-0344).
19. Hill BR, Steed OT. Harsh environmental qualification of cables for use in Sizewell B PWR power station. In: International Conference on Operability of Nuclear Systems in Normal and Adverse Environments; 1989; Lyon, France. Proceedings. Vienna: IAEA; 1989.
20. IAEA: International Atomic Energy Agency. IAEA-TECDOC-1188: assessment and management of ageing of major nuclear power plant components important to safety: in-containment instrumentation and control cables. Vienna: IAEA; 2000. (vol 1).
21. Charlesby A. The effects of ionizing radiation on polymers. In: Clegg DW, Collyer AA, editors. Irradiation effects on polymers. London: Elsevier Applied Science; 1991. p. 39-78.
22. Malkov GV, Demidov SV, Allayarov SR, Nikol'skii VG, Semavin KD, Kapasharov AT, et al. Combined effect of high-temperature shear grinding and gamma-radiation on the thermal properties of polyethylene. High Energy Chem. 2020;54(2):130-5. http://dx.doi.org/10.1134/S0018143920020137.
23. Rahman H, Alimuzzaman S, Sayeed MMA, Khan RA. Effect of gamma radiation on mechanical properties of pineapple leaf fiber (PALF)reinforced lowdensity polyethylene (LDPE)

composites. J Plast Technol. 2019;23(2):229-38. http://dx.doi.org/10.1007/s12588-019-09253-4.
24. Catari E, Albano C, Karam A, Perera R, Silva P, González J. Grafting of a LLDPE using gamma irradiation. Nucl Instrum Methods Phys Res B. 2005;236(1-4):338-43. http://dx.doi.org/10.1016/j.nimb.2005.03.273.
25. Prysmian Group. Afumex green, the first building wire eco cable [Internet]. Milan; 2020 [cited 2020 May 5]. Available from: https://www.prysmiangroup.com/it/node/4516
26. Vyazovkin S. Computational aspects of kinetic analysis: Part C. The ICTAC Kinetics Project - the light at the end of the tunnel? Thermochim Acta. 2000;355(1-2):155-63. http://dx.doi.org/10.1016/S0040-6031(00)00445-7.
27. Starink MJ. The determination of activation energy from linear heating rate experiments: a comparison of the accuracy of isoconversion methods. Thermochim Acta. 2003;404(1-2):163-76. http://dx.doi.org/10.1016/S0040-6031(03)00144-8.
28. Kissinger HE. Reaction kinetics in differential thermal analysis. Anal Chem. 1957;29(11):1702-6. http://dx.doi.org/10.1021/ac60131a045.
29. Akahira T, Sunose T. Transactions of joint convention of four electrical institutes, paper no. 246 (1969) research report, Chiba Institute of Technology. J Sci Educ Technol. 1971;16:22-31.
30. Murray P, White J. Kinetics of the thermal dehydration of clays. Trans Br Ceram Soc. 1955;54:204-38.
31. Ozawa T. Kinetic analysis of derivative curves in thermal analysis. J Therm Anal. 1970;2(3):301-24. http://dx.doi.org/10.1007/BF01911411.
32. Ozawa T. Estimation of activation energy by isoconversion methods. Thermochim Acta. 1992;203:159-65. http://dx.doi.org/10.1016/0040-6031(92)85192-X.
33. Doyle CD. Estimating isothermal life from thermogravimetric data. J Appl Polym Sci. 1962;6(24):639-642. http://dx.doi.org/10.1002/app.1962.070062406.
34. Doyle CD. Series approximations to the equation of thermogravimetric data. Nature. 1965;207(4994):290-1. http://dx.doi.org/10.1038/207290a0.
35. Friedman HL. Kinetics of thermal degradation of char-forming plastics from thermogravimetry. Application to a phenolic plastic. J Polym Sci Polym Symp. 1964;6:183-95.
36. Lyon RE. An integral method of nonisothermal kinetic analysis. Thermochim Acta. 1997;297(1-2):117-24. http://dx.doi.org/10.1016/S0040-6031(97)00158-5.
37. Yang J, Miranda R, Roy C. Using the DTG curve fitting method to determine the apparent kinetic parameters of thermal decomposition of polymers. Polym Degrad Stabil. 2001;73(3):455-61. http://dx.doi.org/10.1016/S0141-3910(01)00129-X.
38. Park JW, Oh SC, Lee HP, Kim HT, Yoo KO. A kinetic analysis of thermal degradation of polymers using a dynamic method. Polym Degrad Stabil. 2000;67(3):535-40. http://dx.doi.org/10.1016/S0141-3910(99)00155-X.
39. Wu CH, Chan CY, Hor JL, Shih SM, Chen LW, Chang FW. On the thermal treatment of plastic mixtures of MSW: pyrolysis kinetics. Waste Manag. 1993;13(3):221-35. http://dx.doi.org/10.1016/0956-053X(93)90046-Y.
40. Conesa JA, Marcilla A, Font R, Caballero JA. Thermogravimetric studies on the thermal decomposition of polyethylene. J Anal Appl Pyrolysis. 1996;36(1):1-15. http://dx.doi.org/10.1016/0165-2370(95)00917-5.
41. ASTM: American Society for Testing and Materials. ASTM D1248-16: Standard specification for polyethylene plastics extrusion materials for wire and cable. West Conshohocken: ASTM; 2016. https://doi.org/10.1520/D1248-16
42. ASTM: American Society for Testing and Materials. ASTM D638-14: Standard test method for tensile properties of plastics. West Conshohocken: ASTM; 2014. https://doi.org/10.1520/D0638-14.
43. Yamamoto T, Minakawa T. The final report of the project of "Assessment of Cable Ageing for Nuclear Power Plants". Tokyo: Japan Nuclear Energy Safety Organization; 2009. (Report; JNES-SS-0903).
44. IEC: International Electrotechnical Commission. IEC/IEEE 62582-2: Nuclear power plants - instrumentation and control important to safety -electrical equipment condition monitoring methods - part 2: indenter modulus. Piscataway: IEEE; 2011.
45. Mishra R, Tripathy SP, Fink D, Dwivedi KK. Activation energy of thermal decomposition of proton irradiated polymers. Radiat Meas. 2005;40(2-6):754-7. http://dx.doi.org/10.1016/j.radmeas.2005.02.022.
46. Dole M, editor. The radiation chemistry of macromolecules. New York: Academic Press; 1972. (vol. I-II).
47. Bracco P, Costa L, Luda MP, Billingham N. A review of experimental studies of the role of free-radicals in polyethylene oxidation. Polym Degrad Stabil. 2018;155:667-83. http://dx.doi.org/10.1016/j.polymdegradstab.2018.07.011.
48. Silverstein RM, Werbster FX. Spectrometric Identification of Organic Compounds. New York: John Wiley & Sons; 1998.
49. IAEA: International Atomic Energy Agency. Assessing and managing cable ageing in nuclear power plants. Vienna: IAEA; 2012. (Nuclear Energy Series; NP-T-3.6).
50. Bartoníček B, Hnát V, Plaček V. Assessment of the insulation degradation of cables used in nuclear power plants. Nucl Instrum Methods Phys Res B. 1999;151(1-4):423-6. http://dx.doi.org/10.1016/S0168-583X(99)00149-4.